ICARUS 93, 174–178 (1991)

NOTE

Simulation of the Spectral Content of the 7.8-μm Emission from Jupiter at High Resolution

RANGASAYI HALTHORE

ST Systems Corporation, Lanham, Maryland 20706

AND

DAVID KRATZ

USRA, NASA GSFC, Greenbelt, Maryland 20771

Received March 1, 1991; revised June 4, 1991

Jovian emission due to $^{12}CH_4$, $^{13}CH_4$, and CH_3D in the 1100 to 1400 cm^{-1} region is simulated at high spectral resolution as seen from the Earth from an altitude of 4 km above sea level. Due to absorption in the Earth's atmosphere, strong lines do not contribute significantly to the total intensity in this region; it is the weak to marginally strong lines that contribute most. Polar hot spots and other midlatitude features observed in broadband observations are conclusively shown to be stratospheric effects. Signal enhancement in the broadband observations is obtained at zenith angles close to zero and increased doppler shifts; however, the magnitude in the latter case is a sensitive function of the stratospheric temperature.

Introduction. Information from the upper parts of a planetary atmosphere, contained in the line cores of an absorbing molecule, is degraded in broadband observations because of averaging over the line wings that are formed much deeper. This is because the energy contained in the line cores is a small fraction of the total energy especially for observations in the "thermal" infrared. High resolution observations and analysis that resolve the lineshape are necessary to extract information from the very upper parts of the planetary atmosphere. Furthermore, if the gases whose emissions are being simulated for observations from a ground-based observatory are present in the Earth's atmosphere as well, absorption and emission in the Earth's atmosphere must be taken into account for a complete simulation or analysis. Problems of telluric methane absorption in the broadband observations have been reported (Caldwell *et al.* 1987). High spectral resolution observations, which are at present possible only from large ground-based telescopes, require the type of analysis that is presented here.

Of particular interest is the 7.8-μm emission from Jupiter. Apart from establishing the presence of a stratosphere due to limb brightening in this band (Gillett and Westphal 1973), the emissions have been used to derive the temperature of the stratosphere (Orton 1977, Kim *et al.* 1985). Broadband observations using the NASA Infrared Telescope Facility (IRTF) at Mauna Kea have revealed what is perhaps the most striking aspect of these emissions—the infrared polar bright spots first observed by Caldwell *et al.* (1980). The north polar hot spot, fixed in magnetic coordinates for a period of more than 10 years, is the focus of multidisciplinary investigations ranging from radio wavelengths to X-rays. Theoretical analyses using Voyager IRIS spectra of the hydrocarbon emissions (Halthore *et al.* 1988), and ground-based observations of hydrogen quadrupole lines (Kim *et al.* 1990) and H_3^+ emissions (Drossart *et al.* 1989, Maillard *et al.* 1990) at wavelengths other than 7.8 μm, indicate that the temperatures in the upper stratosphere may be very high. Thus, contribution to line cores in the hydrocarbon emissions in the hot spot may be significant. The present analysis reveals the nature of the emissions at a spectral resolution of 0.005 cm^{-1} in the region bracketed at the lower end at 1100 cm^{-1} by atmospheric ozone absorption and at the higher end at 1400 cm^{-1} by atmospheric water vapor absorption.

Results and discussion. For the Jovian atmospheric simulation we use the temperature–pressure profile presented in Table 1 (14 levels), and a hydrogen–helium atmosphere containing 2000 ppmv of $^{12}CH_4$, 20 ppmv of $^{13}CH_4$, and 350 ppbv of CH_3D. The abundance of methane is allowed to decrease with altitude as required by gravitational separation and photochemical destruction. At a pressure of 1 μbar for example, methane abundance is conservatively taken to be 10 ppmv (R. Gladstone, private communication). Simulation is also performed at a "hot" upper stratospheric temperature of 220 K estimated as a lower limit for the temperature of the hot spot by Halthore *et al.* (1988). The temperature refers to an "isothermal" region above an altitude corresponding to 5 mbar (Table 1). The simulation employs a line-by-line procedure which utilizes the 1986 AFGL HITRAN database (Rothman *et al.* 1987) for molecular line parameters and the Voigt profile for lineshapes. H_2 opacity is calculated as outlined in Borysow *et al.* (1985).

The terrestrial atmospheric simulation uses the temperature–pressure profile and water vapor abundance profile which are specified by the McClatchey *et al.* (1972) tropical atmosphere (30 levels), and a nitrogen–oxygen atmosphere containing 175 ppmv of $^{12}CH_4$, 1.8 ppmv of $^{13}CH_4$, and 1 ppbv of CH_3D. An altitude of 4 km is used to simulate observing from Mauna Kea. LTE is assumed and spectra are generated at varying spectral resolution ranging from 0.02 cm^{-1} to 0.001 cm^{-1}, which is less than the doppler width of methane lines and three doppler

0019-1035/91 $3.00

TABLE I

Temperature (K)	Pressure (bars)	Methane (mole fraction)
170.0	1.00	2.0×10^{-3}
137.0	0.50	2.0×10^{-3}
111.0	0.20	2.0×10^{-3}
109.0	0.15	2.0×10^{-3}
111.0	0.10	2.0×10^{-3}
127.0	0.05	2.0×10^{-3}
145.0	0.02	2.0×10^{-3}
150.0	0.01	2.0×10^{-3}
158.0	0.005	2.0×10^{-3}
165.0	0.002	2.0×10^{-3}
165.0	0.001	1.8×10^{-3}
165.0	1.0E-04	1.2×10^{-3}
165.0	1.0E-05	3.8×10^{-4}
165.0	1.0E-06	9.8×10^{-6}

shifts corresponding to 0 cm^{-1} and ± 0.1 cm^{-1} which are the extreme cases for Jupiter. The programs are run on an IRIS work station and typically take 40 min cpu.

A simulated Jovian spectrum as seen from the Earth at 0.005 cm^{-1} resolution is shown in Fig. 1. It was obtained by first computing the emission from Jupiter as it would appear at the top of the Earth's atmosphere, followed by a radiative transfer calculation in the Earth's atmosphere down to a level of 4 km (the altitude of Mauna Kea, Hawaii) to yield the combined Earth and Jupiter spectrum. From this the Earth's atmospheric emission spectrum is subtracted to obtain the spectrum shown in Fig. 1. The absence of strong emission lines in the center of the ν_4 band at 1306 cm^{-1} is clearly evident. Instead the line intensities increase toward lower wavenumbers following the Planck function peak corresponding to a stratospheric temperature of 165 K. Strong methane lines near the band center are highly attenuated in the Earth's atmosphere. Even the intermediate strength lines do not show up in this figure as sharp features and it is the weak lines that contribute to the overall appearance of Fig. 1. Toward the shorter wavenumber region the lines are mostly due to CH_3D, whose band center lies at 1161 cm^{-1}.

In Fig. 2, a smaller region from 1205 to 1210 cm^{-1} is expanded to reveal the general composition of the emission: that the emission is made up of sharp features superimposed on a "background" of broad features. In certain parts of the spectrum the broad features reveal absorption due to telluric ozone and nitrous oxide. Much of the energy in the region from 1100 to 1300 cm^{-1} is in the broad features. Intuitively it is obvious that the sharp features are the cores of lines formed in the upper parts of the Jovian atmosphere and the broad features are formed much lower down. This is confirmed in a contribution function analysis shown in Fig. 3. The contribution function used here is defined as $I_i/\Sigma I_i$, with I_i given by

$$I_i = B_i\{1 - \exp(-\tau_i)\} \exp\left(\sum_{j=i+1}^{N} \tau_j\right),$$

where I_i is the contribution to the radiance at the top of atmosphere from the ith layer, B is the Planck function evaluated at the temperature of the ith layer, τ is the optical thickness, and N is the total number of layers plus one. $i = 1$ corresponds to a lower boundary whose optical thickness is very large.

In Fig. 3, curve 3′ corresponds to the emission at the peak of the sharp feature at 1208.6975 cm^{-1} due to methane marked 3′ in Fig. 2. Curves 2′ and 4′ are obtained for emission one step (0.005 cm^{-1}) on either side of the maximum in Fig. 2. Curve 1′ is obtained near the peak of the

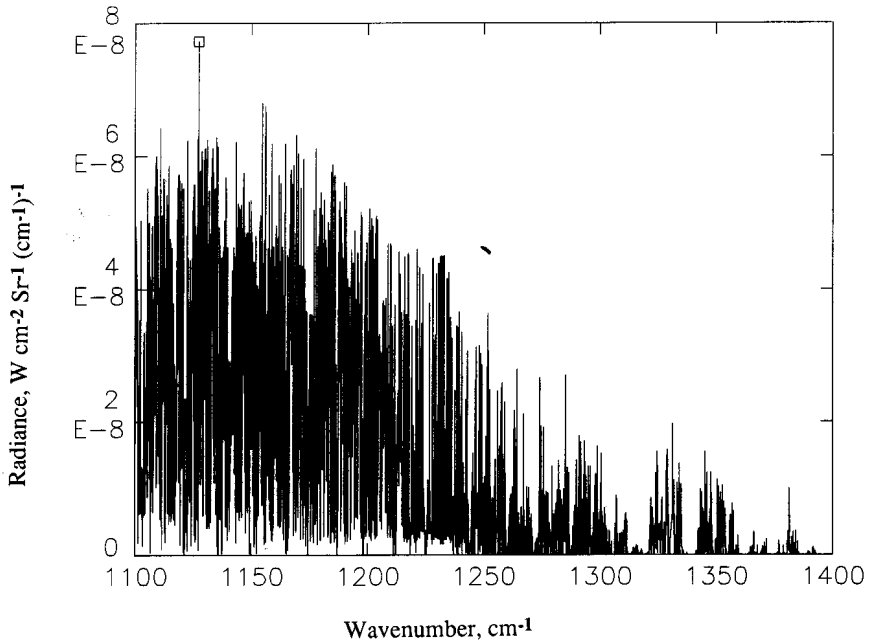

FIG. 1. Jovian emission as seen from an altitude of 4 km above sea level at spectral resolution of 0.005 cm^{-1} and zero doppler shift is shown here. Lack of features at 1306 cm^{-1}, the ν_4 band center, is obvious. Instead, sharp features increase in intensity toward the lower end. The rate of increase is the same as that for a black body at 165 K. The strongest line at 1127.2275 cm^{-1} belongs to CH_3D.

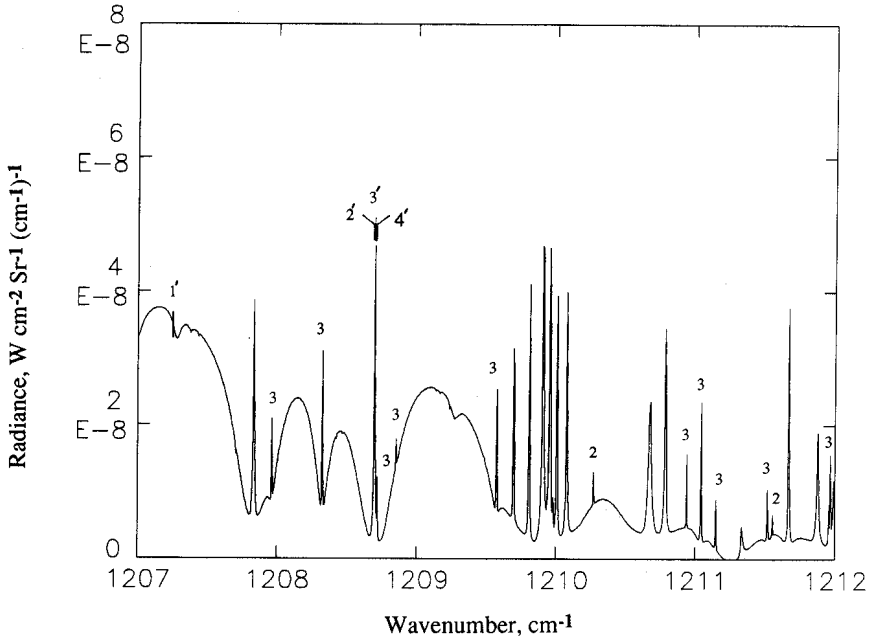

FIG. 2. Same as in Fig. 1, but expanded to reveal the nature of the broad and narrow features. The lines are marked 3 for CH_3D and 2 for $^{13}CH_4$. Those that are left unmarked are due to CH_4 and are seen to be more numerous. A classic emission line profile due to CH_4 is seen centered about 1208.7 cm^{-1} where the line core is in emission, near wing is in absorption, and far wings are in emission. The primed numbers correspond to the contribution curves of the next figure.

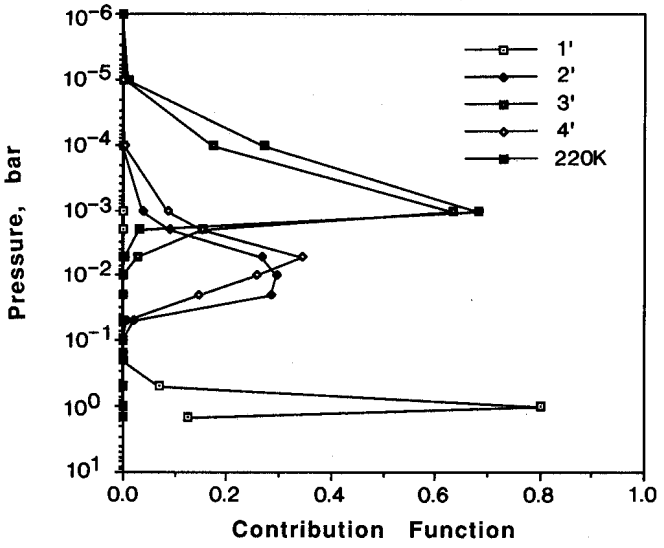

FIG. 3. The contribution functions for the four points marked in the previous figure are shown here. The point marked 3′ is at the very peak of the sharp feature at 1208.6975 cm^{-1} and has contributions from regions as high as 10 μbar. Points 2′ (1208.6925 cm^{-1}) and 4′ (1208.7025 cm^{-1}) are one spectral resolution step away (0.005 cm^{-1}) on either side of 3′ and have contributions from altitudes much deeper but still in the stratosphere. Point 1′ which is near the peak of the broad feature is tropospheric emission. Also shown is a curve for the peak of the sharp feature at 3′ for a stratospheric temperature of 220 K. The contribution curve has shifted upward for this case relative to the "cool" stratospheric case.

broad feature. The line core has significant contribution from altitudes up to 10 μbar. Note that we have used a rather conservative estimate of the upper atmospheric temperature of 165 K. At a temperature of 220 K, the contribution between 10 and 100 μbar can be seen to be higher than that for 165 K. Furthermore, if we assume that the homopause is above the 1 μbar level and use a constant mixing ratio of methane up to 1 μbar, the contribution to the core from above the 10 μbar level becomes significant.

The greatest contribution to the peak of the broad feature is clearly in the troposphere. Figure 2 shows the classic emission/absorption line profile where the line cores are in emission, line wings are in absorption, and the far wings are in emission again due to lower absorption at higher altitudes. Not all the sharp features are cores of lines however. For example, at wavenumbers higher than about 1250 cm^{-1}, partial line wings show up as sharp but asymmetric features.

By forcing the temperature below the tropopause on Jupiter artificially to absolute zero and carrying out the simulation, only the contribution from the Jovian stratosphere is isolated. When this spectrum is subtracted from the total emission shown in Fig. 1, the tropospheric contribution is obtained. The result is shown in Fig. 4. It is significant that above about 1230 cm^{-1}, there is no contribution from the troposphere and even the broad features originate in the stratosphere. Superimposed on this figure is the filter function of a broadband filter used by several investigators (including Caldwell, Orton, and others) on the IRTF to study Jovian stratospheric emissions. Except for a small overlap at the lower end of the band, the broadband observations reported by these investigators were effectively sampling only the stratosphere. Phenomena such as the polar brightenings and midlatitude nonuniformities are all stratospheric effects. Note that this does not preclude the existence of the stratospheric effects on the troposphere or vice versa.

We next investigated the effect of varying doppler shifts on the broadband observations. In the region between 1250 and 1260 cm^{-1}, a range that is typical of the stratospheric emission range, the integrated intensity is 11.3% higher for the +0.1 cm^{-1} shift case compared with the zero

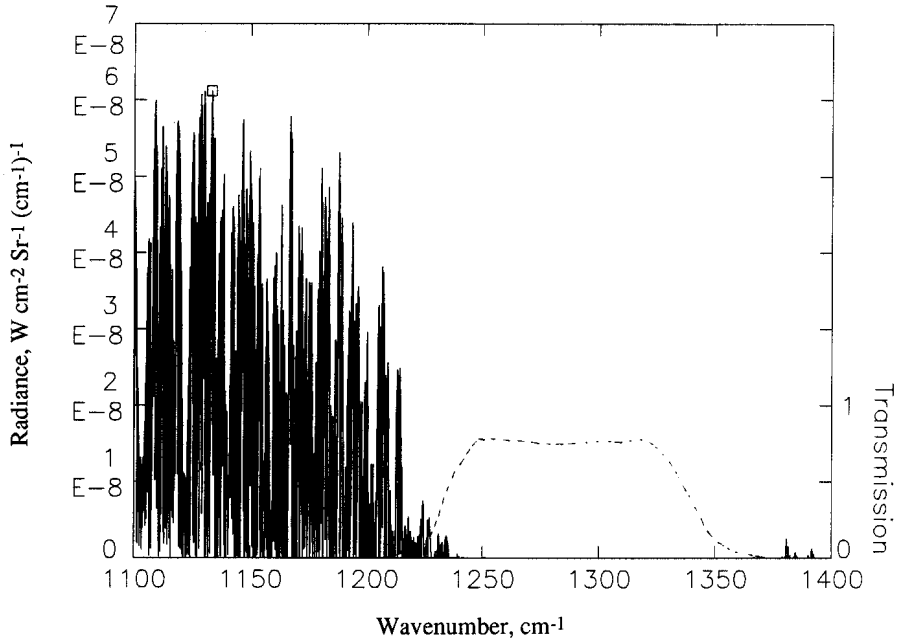

FIG. 4. This figure shows that the tropospheric emission beyond about 1230 cm^{-1} is essentially zero. Thus the emission seen in Fig. 1 from 1230 to 1400 cm^{-1} is from the stratosphere. A broadband filter function used for observations on Mauna Kea, shown here as a dotted line, is sampling essentially the Jovian stratosphere. The features which appear sharp below 1220 cm^{-1} are actually the broad features of Fig. 2.

shift. For the -0.1 cm^{-1} shift, the corresponding increase is about 8%. While this is marginal, at higher stratospheric temperatures, the line intensities increase significantly with doppler shift thus increasing the integrated intensity by a larger amount. For example at 220 K upper stratospheric temperature, the corresponding numbers for ± 0.1 cm^{-1} shifts are 43 and 37%, respectively. Note that the temperature dependence of integrated intensity on the doppler shift has to do with the changing lineshape with temperature and preferential absorption in the cores of lines in the Earth's atmosphere.

In addition to the doppler shift, an important consideration to improve the signal strength is the zenith angle of Jupiter at the time of observation. For the wavenumber range 1250–1260 cm^{-1}, the signal strength at 30° zenith angle is 6% less than at zenith, while the reductions in intensity for zenith angles 60° and 75° are 29 and 54% of the value at zenith. This is more of an effect than the improvement due to doppler shift. At 220 K, the relative loss for 30°, 60°, and 75° zenith angles are 8, 35, and 60%, respectively. Thus the zenith angle effect in this wavenumber range is at least as important as the doppler shift effect.

We next studied the effect of changing spectral resolution. Improving the spectral resolution to 0.001 cm^{-1}, which is of the order of the doppler width of methane lines, does not alter the appearance of Figs. 1 and 2 or the contribution function analysis of Fig. 3. Calculations here were performed at 0.005 cm^{-1} for the entire region mainly to save the computer and graphing resources. Degrading the spectral resolution by a factor of 2 to 0.01 cm^{-1} resulted in minor changes in the intensity of the sharp features. However, at a resolution of 0.02 cm^{-1}, the sharp features were essentially absent except for a few lines. Thus high resolution observations to probe upper parts of the stratosphere must have a resolution better than 0.01 cm^{-1} for observations from 4 km.

The variation of the doppler effect in the field of view due to Jupiter's rotation was not included in this simulation as this is important for the finite spatial resolution/very high spectral resolution observations (Kostiuk *et al.* 1987).

Conclusions. In the 7.8-μm band at spectral resolution better than 0.01 cm^{-1}, ground observations can yield temperature information from the very upper parts of the stratosphere of Jupiter. This information is invaluable for studying the polar hot spots and other stratospheric phenomena. The lines to observe are not the very strong or even the strong lines of $^{12}CH_4$ near the center of the band at 1300 cm^{-1} but rather the weak lines, well away from the band center, around 1200 cm^{-1}, where the line intensities increase due to the shape of the Planck function at the stratospheric temperatures encountered on Jupiter. It is possible to observe simultaneously many lines in a given region due to several species: $^{12}CH_4$, $^{13}CH_4$, and CH_3D, so that D/H ratios can be derived for the stratosphere. The increase in intensity in broadband observations due to increased doppler shift is marginal at low stratospheric temperatures but is significant at higher temperatures. If the observations are performed at a low elevation angle, much of the increased intensity due to the doppler effect will be offset due to the increased path length in the earth's atmosphere. Broadband observations reported previously in the literature in the 7.8-μm band using the IRTF have sampled predominantly the stratosphere and such phenomena as the polar hot spots and the midlatitude wave-like features are undoubtedly stratospheric effects.

ACKNOWLEDGMENTS

We acknowledge Drs. Gordon Bjoraker and Ted Kostiuk of NASA Goddard Space Flight Center, Dr. John Caldwell of York University, Dr. Pierre Drossart of the Paris Observatory at Meudon for useful suggestions and discussions, Dr. Sang Kim of University of Maryland for providing us with the filter bandpass function frequently used in the broadband observations on Mauna Kea, and Dr. Glenn Orton of Jet Propulsion Laboratory for giving us the program to calculate hydrogen opacity.

REFERENCES

BORYSOW, J., L. TRAFTON, L. FROMMHOLD, AND G. BIRNBAUM 1985. Modeling of pressure-induced far-infrared absorption spectra: Molecular hydrogen pairs. *Astrophys. J.* **296,** 644–654.

CALDWELL, J., S. J. KIM, AND R. D. CESS 1987. The influence of telluric methane on infrared observations of planets. *Bull. Am. Astron. Soc.* **19**(3), 874.

CALDWELL, J., A. T. TOKUNAGA, AND F. C. GILLETT 1980. Possible infrared aurorae on Jupiter. *Icarus* **44,** 667–675.

DROSSART, P., J.-P. MAILLARD, J. CALDWELL, S. J. KIM, J. D. G. WATSON, W. A. MAJEWSKI, J. TENNYSON, S. MILLER, S. K. ATREYA, J. T. CLARKE, J. H. WAITE JR., AND R. WAGENER 1989. Detection of H_3^+ on Jupiter. *Nature* **340**(6234), 539–541.

GILLET, F. C. AND J. A. WESTPHAL 1973. Observations of 7.9 micron limb brightening on Jupiter. *Astrophys. J.* **179,** L153–L154.

HALTHORE, R. N., A. BURROWS, AND J. CALDWELL 1988. Infrared polar brightenings on Jupiter. V. A thermal equilibrium model for the north polar hot spot. *Icarus* **74,** 340–350.

KIM, S. J., J. J. CALDWELL, A. R. RIVOLO, R. WAGENER, AND G. S. ORTON 1985. Infrared polar brightenings on Jupiter. III. Spectrometry from the Voyager 1 IRIS experiment. *Icarus* **64,** 233.

KIM, S. J., P. DROSSART, J. CALDWELL, AND J.-P. MAILLARD 1990. Temperatures of the Jovian auroral zone inferred from 2-μm H_2 quadrupole line observations. *Icarus* **84,** 54–61.

KOSTIUK, T., F. ESPENAK, D. DEMING, M. J. MUMMA, AND D. ZIPOY 1987. Spatial distribution of ethane on Jupiter. *Icarus* **72,** 394–410.

MAILLARD, J.-P., P. DROSSART, J. K. G. WATSON, S. J. KIM, AND J. CALDWELL 1990. H_3^+ fundamental band in Jupiter auroral zones at high resolution from 2400 to 2900 cm^{-1}. *Astrophys. J.* **363,** L37–L41.

MCCLATCHEY, R. A., R. W. FENN, J. E. SELBY, F. E. VOLZ, AND J. S. GARING 1972. Optical properties of the atmosphere, *AFCRL Environmental Research Paper,* 3rd ed., No. 411, 108 pp.

ORTON, G. S. 1977. Recovery of the mean Jovian temperature structure from inversion of spectrally resolved thermal radiance data. *Icarus* **32,** 41–57.

ROTHMAN, L. S., R. R. GAMACHE, A. GOLDMAN, L. R. BROWN, R. A. TOTH, H. M. PICKETT, R. L. POYNTER, J.-M. FLAUD, C. CAMY-PEYRET, A. BARBE, N. HUSSON, C. P. RINSLAND, AND M. A. H. SMITH 1987. The HITRAN database, 1986 edition. *Appl. Opt.* **26,** 4058–4097.